Available online at www.sciencedirect.com
SCIENCE DIRECT®
International Journal of Heat and Mass Transfer 47 (2004) 1247–1255
International Journal of HEAT and MASS TRANSFER
www.elsevier.com/locate/ijhmt

A dual reciprocity BE-based sequential function specification solution method for inverse heat conduction problems

A. Behbahani-nia, F. Kowsary *

Department of Mechanical Engineering, Faculty of Engineering, University of Tehran, Tehran, Iran

Received 15 December 2002; received in revised form 10 September 2003

Abstract

In this work, a method based on the Dual Reciprocity Boundary Element along with Sequential Function Specification scheme is suggested for solving two-dimensional inverse heat conduction problems involving unknown time and space varying boundary heat flux estimation. The measured transient temperature data utilized in the solution may be from locations inside the body or from locations on its inactive boundaries. The spatial variation of the unknown heat flux is approximated using polynomials, which is shown to conveniently reduce the number of unknowns in the inverse algorithm. The effectiveness and the reliability of the method are verified via a set of test data obtained by simulated experiments, which take into consideration various boundary heat flux characteristics.

Keywords: Boundary element; Dual reciprocity; Inverse; Conduction; Sequential

1. Introduction

Inverse heat conduction problems (IHCP) have recently found wide applications in industries. These applications are categorized as identification, design, and control problems [1]. More specifically, IHCP involves estimation of surface boundary conditions, thermophysical properties, or volumetric heat generation using some temperature data collected from locations within or on the surfaces of the body.

Any IHCP algorithm, regardless of its theoretical approach, requires the usage of a well-established solution routine for direct heat conduction calculations. This solution routine may be called upon numerous times by the main IHCP computational routine. Therefore, use of a highly efficient as well as accurate direct calculation schemes is essential in any IHCP code. Different numerical methods including the finite difference, the finite element, and the boundary element methods have been used as computational tools for direct discretization in IHCP. Amongst these methods, the BEM reduces problem dimensionality by one, which clearly saves computational time and memory. In fact by bypassing the normally complex internal grid generation process, the BEM is particularly adaptable for analyzing irregularly shaped bodies as is desired in many practical applications. Flexibility of choosing thermocouple locations within the body is the other advantage of using BEM in IHCP.

Due to these computational advantages, the boundary element method has increasingly received greater attention in recent years. Application of BEM for steady problems is straightforward, and the theories are well established [2]. The unsteady problems are, however, much more difficult to deal with using the BEM even though several methods have been developed in this regard. Some of these methods require domain integration, which causes the main advantage of the BEM; i.e. elimination of the domain discretization, to be lost. Two *boundary only form* methods, which have received greater attentions, are the Dual Reciprocity and the

* Corresponding author. Fax: +98-21-8013029.
E-mail addresses: behbahan@chamran.ut.ac.ir (A. Behbahani-nia), fkowsari@chamran.ut.ac.ir (F. Kowsary).

0017-9310/$ - see front matter
doi:10.1016/j.ijheatmasstransfer.2003.09.023

Nomenclature

$\mathbf{A}$	$m \times 1$ matrix of unknown coefficients
$\mathbf{C}$	$n \times m$ matrix
d	constant amplitude
$f(r)$	coordinate function
G	fundamental solution of Laplace equation
m	the number of unknown coefficient
m_k	degree of polynomial
N	the number of boundary points
N_p	the total number of points (boundary and Dual Reciprocity points)
Nu	Nusselt number
n	the number of heat flux components or normal direction
n_t	the number of thermocouples
$\mathbf{P}$	$N_p \times N_p$ matrix
p	the number of segments or a random number between 0 and 1
q	heat flux
q_{ex}	exact heat flux
q_{es}	estimated heat flux
$\mathbf{R}$	$N_p \times N$ matrix
r	the number of future time steps
r_j	distance to the source point
$\mathbf{S}$	$N_p \times N$ matrix
s	spatial variable
T	temperature
t	time
$\mathbf{W}$	diagonal weighting matrix
x	spatial variable
y	spatial variable
Y	measured temperature
Z	sensitivity coefficient

Greek symbols

α	arbitrary real constant used in Eq. (2)
β	interpolating coefficient
η	relative percentage error
Δl	boundary element length
Δt	time step
λ	shape coefficient
Ω	two-dimensional surface domain
Γ	boundary of Ω

Subscripts

i, j, k	indices for time, thermocouples, nodes, heat flux components, or segments
M	time index

so-called Convolution method. The latter method employs a time dependent fundamental solution in which, in order to avoid the domain integration, one is forced to restart the time integration from the initial condition for each time step calculation. All of the temperatures and related coefficients should be kept in memory to perform this integration at each time step. This makes the technique time and memory consuming if the number of time steps is large, even though the method has a boundary only character [3]. The former method, developed later, eliminates this difficulty by using the fundamental solution of the Laplace equation. In this method the time derivative term, treated as a source, is transferred to the boundary by using the Dual Reciprocity Method [4]. The method was first developed for linear problems but later was extended successfully to different kinds of nonlinear problems involving temperature dependence thermal properties using the kirchhoff transformation [4–6].

Most of previous applications of BEM in inverse heat conduction have been concerned with time-dependent fundamental solution method (i.e., the convolution approach). Kurpisz and Nowak proposed an IHCP algorithm using a combination of the Sequential Function Specification and regularization methods [7]. Chantasiriwan used the Sequential Function Specification without extra (Tikhonov) regularization [8]. Lesnic, Elliott and Ingham proposed a whole domain method based on minimizing kinetic energy for solving a one-dimensional problem [9]. Huang and Chen used the conjugate gradient method for irregular shapes [10]. Finally, Pasquetti and Niliot utilized Tikhonov regularization [11].

In this work the major concern is combining the Dual Reciprocity BEM and the Sequential Function Specification method for estimation of unknown boundary heat flux in a two-dimensional configuration. Sequential algorithms have the advantage of being highly efficient, as compared to the whole domain methods, without a significant loss in accuracy [12]. A thorough search in the existing literature has revealed that the only reported work, which has utilized the Dual Reciprocity BEM in conjunction with an IHCP algorithm, is that due to Tanaka and Krishna [13] in their whole domain conjugate-gradient method. However, owing to the popularity and the great utility of the Sequential Function Specification IHCP algorithm, use of the Dual Reciprocity BEM with this algorithm deserves greater attentions.

2. Problem statement

The geometry of a general two-dimensional problem is illustrated in Fig. 1. The boundary condition along Γ_1

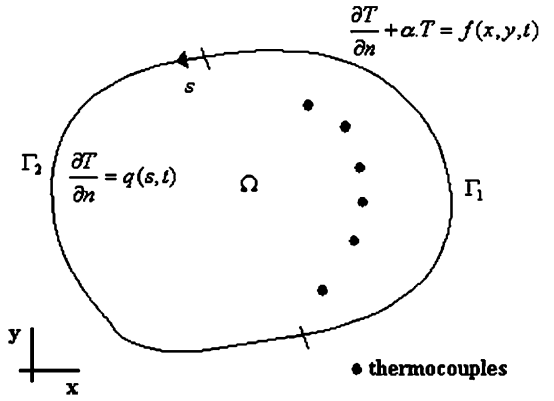

Fig. 1. Geometry of a general two-dimensional problem.

is known, while on Γ_2, it is unknown. This unknown boundary condition could be temperature, heat flux, or convective heat transfer coefficient, although heat flux estimation is the object of the present work.

The governing differential equation along with initial and boundary conditions can be expressed in a dimensionless form as

$$\frac{\partial^2 T}{\partial x^2} + \frac{\partial^2 T}{\partial y^2} = \frac{\partial T}{\partial t} \quad \Omega \tag{1}$$

$$\frac{\partial T}{\partial n} + \alpha T = f(x,y,t) \quad \Gamma_1 \tag{2}$$

$$\frac{\partial T}{\partial n} = q(s,t) \quad \Gamma_2 \tag{3}$$

$$T(x,y,0) = 1.0 \quad \Omega \tag{4}$$

$$Y(x_j,y_j,t_i) = g_j(t_i) \quad j = 1,\ldots,n_t \tag{5}$$

The function $q(s,t)$ is known in a direct problem, but is unknown in an inverse problem and is to be estimated using temperatures measured by sensors located inside the physical domain or on the boundary surfaces described by Eq. (5).

3. Direct solution

The Dual Reciprocity Boundary Element method is used for solving Eq. (1). In this methodology, the time derivative of the temperature is treated as a source term and the fundamental solution of Laplace equation is used as followed

$$G = \frac{1}{2\pi}\mathrm{Ln}(r_j). \tag{6}$$

Using Eq. (6), the weighted integral of Eq. (1) can be given as

$$\int_\Omega G(\nabla^2 T)\,\mathrm{d}\Omega = \int_\Omega GT\frac{\partial T}{\partial t}\,\mathrm{d}\Omega, \tag{7}$$

where Ω defines the domain of integration. Using the Green's second identity Eq. (7) can be written as

$$\lambda T(r_j,t) - \int_\Gamma \left[T\frac{\partial G}{\partial n} - G\frac{\partial T}{\partial n}\right]\mathrm{d}\Gamma = \int_\Omega G\frac{\partial T}{\partial t}\,\mathrm{d}\Omega, \tag{8}$$

where Γ represents the boundary of the domain Ω, and λ is the shape coefficient.

The right hand side of Eq. (8) can now be manipulated by using a secondary interpolation to reduce it to a boundary only form. One may write

$$\frac{\partial T}{\partial t} = \sum_{J=1}^{N_p} f(r_j)\beta_j(t). \tag{9}$$

The function $f(r)$ can be of various types, for example polynomial of any chosen degree, but the following function is found to be the most versatile as shown by computational studies [2]

$$f(r) = 1 + r. \tag{10}$$

A few internal points known as Dual Reciprocity points and boundary points are used for the above interpolation.

By substitution of Eq. (9) into Eq. (8) and performing some mathematical manipulations, which can be found in Ref. [4], one may obtain

$$[\mathbf{R}]\left[\frac{\partial \mathbf{T}}{\partial n}\right] - [\mathbf{S}][\mathbf{T}] = [\mathbf{P}]\left[\frac{\partial \mathbf{T}}{\partial t}\right]. \tag{11}$$

Different methods are used to discretize the time derivative, including one-step, and multi-step θ schemes, and a series of schemes known as least square methods. The accuracy and stability of these schemes as applied to the Dual Reciprocity BEM are compared in several references such as [4,14]. Implicit θ scheme was used in this work due to its simplicity and reported adequate accuracy. Thus

$$\left[\frac{\partial T}{\partial t}\right]^{t+\Delta t} = \frac{1}{\Delta t}[T^{t+\Delta t} - T^t]. \tag{12}$$

Combining Eqs. (11) and (12), one can obtain

$$[\mathbf{S}][\mathbf{T}]^{t+\Delta t} - [\mathbf{R}]\left[\frac{\partial \mathbf{T}}{\partial n}\right]^{t+\Delta t} + \frac{1}{\Delta t}[\mathbf{P}][\mathbf{T}]^{t+\Delta t} - \frac{1}{\Delta t}[\mathbf{P}][\mathbf{T}]^t = 0. \tag{13}$$

Eq. (13) can now be used for solving the direct problem.

Different references have reported presence of a lower stability limit for the time steps. This is usually given in the order of [4]

$$\frac{\Delta t}{(\Delta l)^2} \approx 1, \tag{14}$$

where Δt and Δl denote, respectively, the dimensionless time step and length of elements.

In this work, small time steps were selected in order to resolve the sensitivity coefficients (used in inverse calculations), which show the characteristics of a thermal shock (i.e., a sudden rise in the heat flux with time) more accurately. To suppress round-off errors, the length of elements was used as the characteristic length for nondimesionalizing the heat equation. This selection makes the nondimensional length elements and time steps to be both in the order of unity.

4. Inverse solution

4.1. An overview of the inverse methods

A number of solution techniques have been proposed to treat the ill-posed nature of inverse heat conduction problems, a thorough review of which can be found in Ref. [1]. These methods can in general be separated into sequential and whole domain methods.

Historically, sequential methods were developed in the US while the whole domain methods were developed in Russia. There is some literature about the comparison of various methods [12]. Each of these methods has its own advantages as described below.

The main benefits of sequential methods over their whole domain counterparts are as follows:

(a) The sequential methods can be used in real time mode.
(b) In nonlinear problems due to temperature dependence of thermal properties, sequential methods provide the possibility of temporary linearization of the problem.
(c) Sequential methods require less memory and computational time.

The whole domain methods have their own advantages as well. For example it has been shown that the conjugate gradient method, which is one of the most successful whole domain algorithms, works well in cases where the unspecified boundary condition covers a big fraction of the boundary [10,13]. This method can be used in a sequential manner as well; however, it loses most of its advantages when it is employed sequentially [15].

Sequential Function Specification method was proposed by Beck [16] for one-dimensional problems and was later developed for two-dimensional problems [17,18]. This method can be improved, as is shown in this paper, in the case of a large number of unknown heat flux components by using piece-wise polynomials, which automatically reduces the number of unknowns or using a combination of Sequential Function Specification and space Tikhonov regularization [18]. The combined Sequential Function Specification and regularization is appropriate for cases where there is a large and sharp variation in spatial distribution of surface heat flux or when there are a relatively large number of parameters to be determined as compared to the number of sensors [18].

4.2. Sequential function specification method

To estimate a space and time varying heat flux function, the active surface is broken up into "n" elements, each with a constant heat flux component. It is temporarily assumed that heat flux components are constant over "r" future time steps, i.e.,

$$\mathbf{q}_M = \mathbf{q}_{M+1} = \cdots = \mathbf{q}_{M+r-1}, \tag{15}$$

where vector $\mathbf{q}_j$ is defined as

$$\mathbf{q}_j^{\mathrm{T}} = [q_j(1), q_j(2), \ldots, q_j(n)]. \tag{16}$$

The objective function to be minimized in order to estimate $\boldsymbol{q}_M$ is defined as

$$S = \sum_{j=1}^{n_t} \sum_{i=1}^{r} W_{i,j}[Y_{j,M+i-1} - T_{j,M+i-1}(\mathbf{q}_M)]^2, \tag{17}$$

where, according to [18], using a Taylor expansion of the calculated temperatures about $\mathbf{q}^*$, which in essence is an initial guess for the unknown heat flux component, we would have

$$T_{j,M+i-1}(\mathbf{q}_M) = T_{j,M+i-1}(\mathbf{q}^*) + \sum_{k=1}^{n} Z_{j,i,k}(q_M(k) - q_M^*(k)), \tag{18}$$

and

$$Z_{j,i,k} = \frac{\partial T_{j,M+i-1}}{\partial q_M(k)} \tag{19}$$

is the sensitivity coefficient. The value of "$\mathbf{q}^*$" is usually set equal to zero or equal to "$\mathbf{q}_{M-1}$".

It is sometimes possible to replace the spatial variation of the heat flux over the entire or part of the active surface by using a polynomial fit. This spatial estimation decreases the number of unknown components, which improves stability of the inverse solution. The heat flux imposed on the active surface is split into spatial segments, each represented by a constant or nth order polynomial with time dependent coefficients. The degree of polynomial to be chosen is at the discretion of the analyst, and depends on a priori estimate of the spatial variation of the heat flux. For cases considered in this

work a second order polynomial appeared to provide sufficiently accurate results.

Thus the function $q(s,t)$, in Eq. (3), may be written as

$$q(s,t) = \sum_{k=1}^{p} \phi_k(s,t), \tag{20}$$

where ϕ_k is a m_kth degree polynomial along the kth segment and zero elsewhere. That is

$$\phi_k(s,t) = a_k(m_k)s^{m_k} + a_k(m_k-1)s^{m_k-1} + \cdots + a_k(0), \quad s_k < s < s_{k+1} \tag{21}$$

and

$$m = \sum_{k=1}^{p} m_k + p. \tag{22}$$

The parameter "m" is the total number of unknown time dependent coefficients.

Using the definitions given above, the system of equations for the unknown heat flux may be written in matrix form as

$$[\mathbf{q}]_{n\times 1} = [\mathbf{C}]_{n\times m}[\mathbf{A}]_{m\times 1}, \tag{23}$$

where "**A**" is the matrix of unknown coefficients defined as

$$\mathbf{A}^{\mathrm{T}} = [\mathbf{A}(\mathbf{1}), \mathbf{A}(\mathbf{2}), \ldots, \mathbf{A}(\mathbf{p})], \tag{24a}$$

$$\mathbf{A}^{\mathrm{T}}(\mathbf{k}) = [a_k(0), \ldots, a_k(m_k)], \tag{24b}$$

and matrix [**C**] is found from Eq. (21).

The weighted least squares norm may be written in matrix form using Eq. (23)

$$S = [\mathbf{Y} - (\mathbf{T}(\mathbf{q}^*) + \mathbf{ZC}(\mathbf{A} - \mathbf{A}^*))]^{\mathrm{T}}\mathbf{W}[\mathbf{Y} - (\mathbf{T}(\mathbf{q}^*) + \mathbf{ZC}(\mathbf{A} - \mathbf{A}^*))]. \tag{25}$$

Minimizing S with respect to **A** gives

$$\mathbf{A} = \mathbf{A}^* + [(\mathbf{Z}^{\mathrm{T}}\mathbf{WZ})\mathbf{C}]^{-1}\mathbf{Z}^{\mathrm{T}}\mathbf{W}(\mathbf{Y} - \mathbf{T}^*). \tag{26}$$

The above equation is used sequentially to estimate matrix "**A**", which in turn, is used to determine $\mathbf{q}_M$ using Eq. (23).

5. Numerical results

Two simulated numerical experiments were used to demonstrate accuracy and stability of the method. In the absence of an exact analytical solution and to avoid a "biased" inverse estimate, the finite difference method (instead of BEM) was used to generate the numerically simulated experimental data. This ensures independency of the estimation to the method used to produce measurement data.

In order to make the situation even more realistic, simulated measured temperatures are perturbed by a random function as follows [1];

$$Y = T + d(1 - 2p). \tag{27}$$

The amplitude of the error, d, is varied to evaluate the quality of the inverse estimator and the sensitivity of the inverse solution to temperature measurement errors.

To measure the accuracy of the inverse solution, the relative percentage error is defined as follows

$$\eta = \frac{\|q_{\mathrm{ex}} - q_{\mathrm{es}}\|_{\mathrm{r.m.s.}}}{\|q_{\mathrm{ex}}\|_{\mathrm{r.m.s.}}} \times 100, \tag{28}$$

where $|\cdot|_{\mathrm{r.m.s}}$ denotes the r.m.s. of a time dependent function and is defined in Ref. [19].

5.1. Test case1

The geometry of the problem and the position of thermocouples are illustrated in Fig. 2. The boundary conditions imposed along S_1, S_2 and S_3 (i.e., inactive surfaces) are all adiabatic. The spatial variation of the heat flux along S_4 is modeled by three heat flux components, the temporal characters of which are shown in Fig. 3. This test case demonstrates the estimation of a spatially distributive heat flux by approximating it with independent components. Two arrangements of thermocouples are considered in this problem. In the first arrangement, denoted by $C1$, the thermocouples are all located on the adiabatic surface opposite to the active one; while in the second arrangement ($C2$), they are located close to the active surface. In this problem, the matrix "**C**" in Eq. (23) can be found easily by considering three segments ($p = 3$) with constant heat flux distributions.

The estimated and exact values for two error amplitudes of ($d = 0.02$ and 0.04) using thermocouple

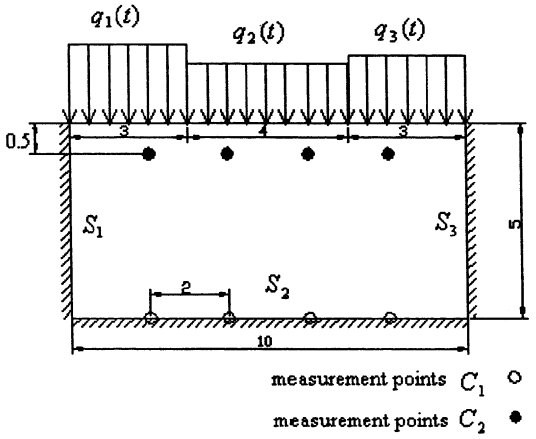

Fig. 2. Geometry and position of thermocouples for the first test case.

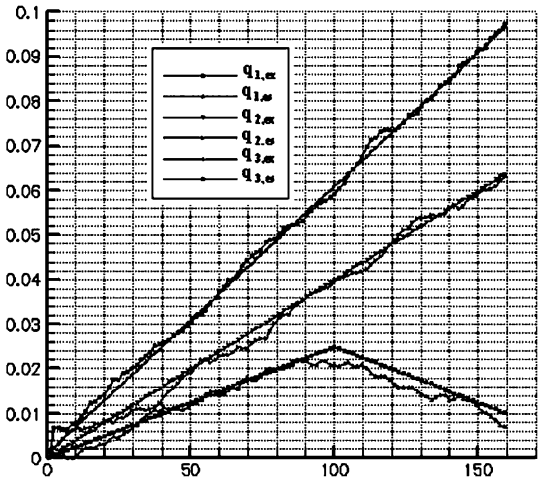

Fig. 3. Estimated and exact heat flux components for the first test case and thermocouples arrangement ($\Delta t = 1.6$, $r = 10$, $d = 0.02$).

arrangement $C2$ are compared in Figs. 3 and 4. Results show a fairly accurate estimation for the duration in which the heat flux is imposed, except for a reduction of the accuracy nearby and after discontinuity for the third heat flux component.

Tables 1 and 2 compare the percent error norm of the second heat flux component for the two thermocouples arrangements. The comparison is made for increasing values of the error amplitude, d. Comparison clearly demonstrates the well-known "damping effect" in IHCP as the sensitivity to measurement errors is increased visibly for the thermocouple arrangement $C1$ which is

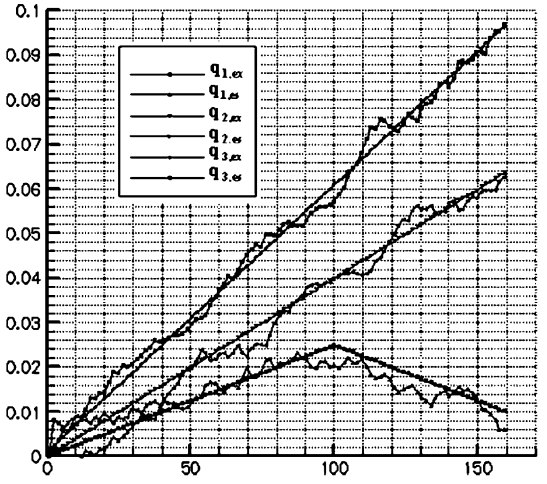

Fig. 4. Estimated and exact heat flux components for the first test case and $C2$ thermocouples arrangement ($\Delta t = 1.6$, $r = 10$, $d = 0.04$).

Table 1
The effect of measurement errors on the solution for the first test case with $C1$ thermocouple arrangement ($\Delta t = 1.6$, $r = 15$)

d	0	2×10^{-3}	0.02	0.04	0.1
η_2	2.85	4.31	26.78	52.63	136.36

Table 2
The effect of measurement errors on the solution for the first test case with $C2$ thermocouple arrangement ($\Delta t = 1.6$, $r = 10$)

d	0	2×10^{-3}	0.02	0.04	0.1
η_2	2.41	2.48	4.21	6.98	16.01

far from the active surface. Nonetheless, the error norm is still within an acceptable engineering range (i.e., less than approximately five percent) for error amplitudes of 2×10^{-3}, and less, for this thermocouple arrangement. The error norm for the thermocouple arrangement $C2$ is satisfactory for all error amplitudes considered except $d = 0.1$. It should be mentioned this is a relatively high value for the error amplitude. The simulated test (i.e., "measurement") data show a maximum thermocouple temperature of 2.18 which means error amplitude of ($d = 0.1$) is about 5% of this maximum "measured" temperature. This relatively high error value affects the data particularly in the beginning of the estimation in which the "measured" temperatures have small values and during which this error amounts to almost 10% of the measured temperature level.

The effect of the number of future data, r, for two error amplitudes is shown in Table 3. As is seen, the results are generally improved by increasing the number of future data. The effect of increasing the number of future data is to reduce the sensitivity to noise and, at the same time, to increase the deterministic bias errors. It is seen, however, that increasing the number of r has a clear improving effect on data having high noise levels, i.e. $d = 0.1$, whereas its effect on data with lower noise level is not as apparent; in fact as going from $r = 10$–15 the value of error norm has increased which should be attributed to increasing the deterministic bias error. Therefore, one can conclude from these results that the optimum value of the number of future time steps depends on amplitude of the measurement errors. For higher noise levels, more future data are required to damp oscillation and to get a stable solution.

Table 3
The effect of number of future time steps on the solution for the first test case with $C2$ thermocouple arrangement ($\Delta t = 1.6$)

d	0.1			0.02		
r	8	10	15	8	10	15
η_2	18.21	16.01	11.82	4.28	4.21	4.60

In a problem with sharp heat flux variations (spatially), the use of more components may become necessary. The difficulty of this type of problem is due to the fact that the sensitivity coefficients become *correlated*, as small differences in adjacent heat flux components are not differentiated by the thermocouples. One such case was considered by Krishna and Tanaka [13], where despite limiting the noise levels to a value as low as 0.1% of maximum temperature, they had to place the thermocouples close to the active surface in order to be able to resolve and estimate the heat flux components. The test case that follows next suggests a possible remedy for this difficulty.

5.2. Test case2

In this test case, it is shown how a polynomial can be used to estimate the spatial variation of the unknown boundary condition by reducing the number of unknown components and, therefore, the sensitivity of the solution to the thermocouples' locations. The geometry and location of the thermocouples are the same as the previous test case except that in this case a Robin boundary condition is imposed on surface S_4, i.e., the active surface (Fig. 5). The spatially varying Nusselt number is calculated, using the suggested correlation in Ref. [20] for a jet impinging on a surface.

Ten heat flux components, which are distributed on the active surface by a second order polynomial, are used to estimate the spatial distribution of heat flux. The total number of unknowns ("m") is three while the number of heat flux components "n" is 10. Once again matrix "**C**" in Eq. (23) can be determined in a straightforward manner.

In Fig. 6 the estimated heat flux on ($x = 4.5$) is compared with exact values (i.e., those obtained from the direct solution) for two different noise levels. For the lower noise level ($d = 0.001$), the estimated heat flux corresponds to the exact value very closely. For higher noise levels ($d = 0.01$) the estimated heat flux gyrates more noticeably, although in a controlled manner, about the exact values.

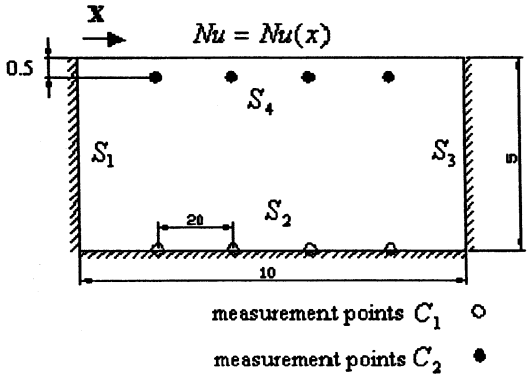

Fig. 5. Geometry and position of thermocouples for the second test case.

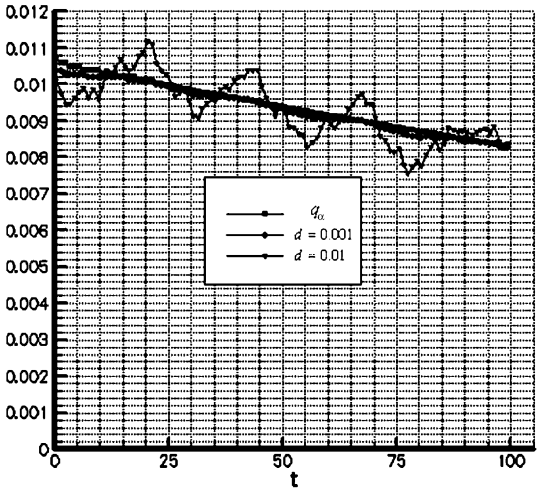

Fig. 6. Comparison of estimated heat flux and heat flux calculated by direct solution for the second test case and $C2$ thermocouples arrangement ($\Delta t = 1.0$, $r = 12$, $x = 4.5$).

The spatial distributions of estimated heat flux at time $t = 20$ obtained by using a second order polynomial approximation are presented in Figs. 7 and 8 for the same two noise levels as in Fig. 6. Once again results show that the method is able to predict the spatial distribution of the heat flux accurately. In particular, the results of Fig. 8, which is for a low error amplitude, show that a second order polynomial can estimate the

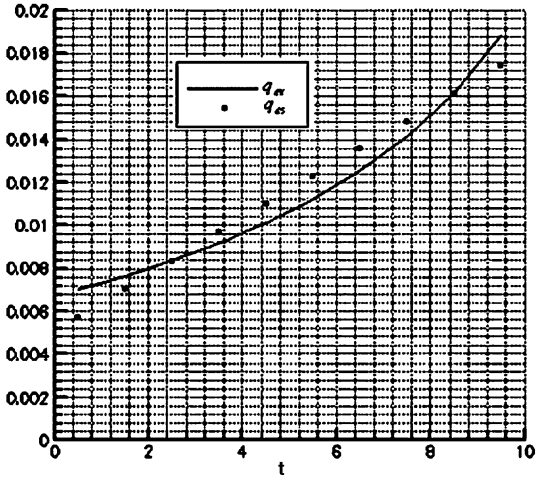

Fig. 7. Comparison of spatial distribution of estimated heat flux and heat flux calculated by direct solution, the second test case with $C2$ thermocouples arrangement ($\Delta t = 1.0$, $r = 12$, $d = 0.01$, $t = 20$).

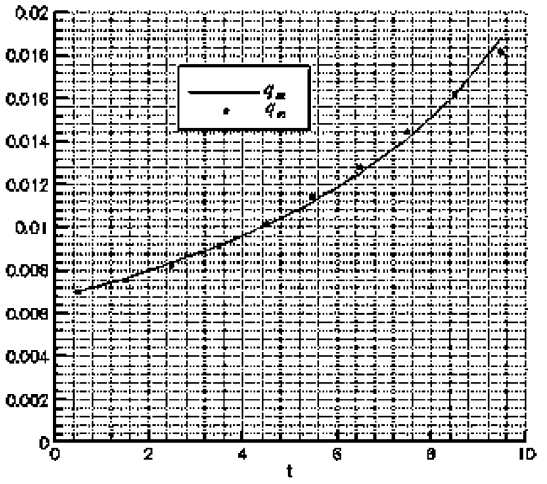

Fig. 8. Comparison of spatial distribution of estimated heat flux and heat flux calculated by direct solution, second test case with $C2$ thermocouples arrangement ($\Delta t = 1.0$, $r = 12$, $d = 10^{-3}$, $t = 20$).

spatial distribution of heat flux without causing a high value of bias error. The estimated heat flux distribution shown in Fig. 8, is on the most part within 8% of the exact value except at one of the ends ($x = 0.5$) where the error is as high as 18%. Seemingly, due to the error in estimation of unknown coefficients, the polynomial does not approximate the exact heat flux at this corner accurately. The difficulty of estimating the heat flux near corners, has also been reported by previous investigators who have broken up the unknown heat flux distribution into independent components [21].

Table 4
The effect of measurement errors on the solution for the second test case with $C1$ thermocouple arrangement ($\Delta t = 1.0$, $r = 12$)

d	0	10^{-3}	0.01	0.02	0.05
η	5.68	7.78	53.89	107.38	268.22

Table 5
The effect of measurement errors on the solution for the second test case with $C2$ thermocouple arrangement ($\Delta t = 1.0$, $r = 12$)

d	0	10^{-3}	0.01	0.02	0.05
η	0.72	0.972	5.79	11.41	28.34

The norms of error for two thermocouple locations are presented in Tables 4 and 5. Again, from the results in Table 4, it is seen the method fails when the thermocouples are far from active surface except for low values of noise level (i.e., $d = 10^{-3}$). When placing the thermocouples close to the active surface, the results become satisfactory except for ($d = 0.05$) which is a relatively high error amplitude as discussed previously.

The effect of the size of the time step for two different number of future data parameters of $r = 6$ and 12 are shown in Table 6. This table in fact shows the effect of the size of the steps of the Fourier number (as the problem was originally posed in a dimensionless form), which also includes the effects of the thermal diffusivity of the material. Considering the *lagging effect* in IHCP, the size of the time step is another control parameter (in addition to r) that can be used in search of the optimum heat flux. By referring to Table 6 it can be seen that for $r = 6$ the optimum solution is achieved by $\Delta t = 2.0$, while for $r = 12$, the optimum is achieved by $\Delta t = 1.0$. In fact if there is a limit in the number of future data, one has to use a bigger step size in time which, in some cases, may cause unwanted bias errors. From the thermal diffusivity perspective, these results show that materials with smaller thermal diffusivity require a bigger time step, which is due to the well-known lagging effect as there would be a larger delay in sensing the imposed heat flux by the thermocouples.

6. Conclusion

A scheme based on the Dual Reciprocity Boundary Element along with Sequential Function Specification method was used successfully for solving two-dimensional inverse heat conduction problems. Two test cases were considered, and the suggested scheme was able to perform the estimation accurately for data noise levels of up to 2% of the maximum measured temperature, if the thermocouples were placed close to the active surface. This level of performance is within the range of what is expected from a direct discretization method; not including the efficiency of the Dual Reciprocity BEM in direct calculations as compared to other discritization schemes. Of course, to achieve accurate inverse estimations beyond these limits, additional regularization may be required, due to the lagging and damping effect of the IHCP; as this would have been required if any other solution technique was used for direct calculations. It

Table 6
The effect of time step on the solution for the second test case with $C2$ thermocouple arrangement ($d = 0.01$)

r	6					12				
Δt	0.1	0.2	0.5	1.0	2.0	0.1	0.2	0.5	1.0	2.0
η	39.78	20.62	11.46	9.46	9.16	15.16	9.80	6.56	5.79	6.16

was also shown, via an example, that approximating the heat flux distribution by an appropriate polynomial, instead of using a large number of heat flux components, could make the inverse estimation more efficient, although further investigation may be necessary in this regard.

References

[1] K. Kurpisz, A.J. Nowak, Inverse Thermal Problems, Computational Mechanics Publications, Souhampton, USA, 1995.

[2] P.A. Ramachandran, Boundary Element Methods in Transport Phenomena, Computational Mechanics Publications, 1994.

[3] R. Pasquetti, A. Caruso, L.C. Wrobel, Transient problems using time-dependent fundamental solution, in: L.C. Wrobel, C.A. Brebbia (Eds.), Boundary Element Methods in Heat Transfer, Computational Mechanics Publications, Boston, 1992, Chapter 2.

[4] C.A. Brebbia, A.J. Nowak, Solving heat transfer problems by the dual reciprocity BEM, in: L.C. Wrobel, C.A. Brebbia (Eds.), Boundary Element Methods in Heat Transfer, Computational Mechanics Publications, Boston, 1992, Chapter 1.

[5] L.C. Wrobel, C.A. Brebbia, The dual reciprocity boundary element formulation for nonlinear diffusion problems, Computer Methods in Applied Mechanics and Engineering 65 (1987) 147–164.

[6] K.M. Singh, M. Tanaka, Dual reciprocity boundary element analysis of nonlinear diffusion: temporal discretization, Engineering Analysis with Boundary Elements 23 (1999) 419–433.

[7] K. Kurpisz, A.J. Nowak, BEM approach to inverse heat conduction problems, Engineering Analysis with Boundary Elements 10 (1992) 291–297.

[8] S. Chantasiriwan, An algorithm for solving multi dimensional inverse heat conduction problem, International Journal of Heat and Mass Transfer 44 (2001) 3823–3832.

[9] D. Lesnic, L. Elliott, D.B. Ingham, Application of the boundary element method to inverse heat conduction problems, International Journal of Heat and Mass Transfer 39 (7) (1996) 1503–1517.

[10] C.-H. Huang, C.-W. Chen, A boundary-based inverse problem in estimating transient boundary conditions with conjugate gradient method, International Journal of Numerical Methods in Engineering 42 (1998) 943–965.

[11] R. Pasquetti, C.Le. Niliot, Boundary element method for solving inverse heat conduction problems: application to a bidimensional transient numerical experiment, Numerical Heat Transfer Part B: Fundamentals 20 (1991) 169–189.

[12] J.V. Beck, B. Blackwell, A. Haji-Sheikh, Comparison of some inverse heat conduction methods using experimental data, International Journal of Heat Mass Transfer 39 (17) (1996) 3649–3657.

[13] K.M. Singh, M. Tanaka, Dual reciprocity boundary element analysis of inverse heat conduction problems, Computer Methods in Applied Mechanics and Engineering 190 (2001) 5283–5295.

[14] K.M. Singh, M.S. Kalra, Time integration in the dual reciprocity boundary analysis of transient diffusion, Engineering Analysis with Boundary Elements 18 (1996) 73–102.

[15] K.J. Dowding, J.V. Beck, A sequential gradient method for the inverse heat conduction problem (IHCP), ASME Journal of Heat Transfer 121 (1999) 300–306.

[16] J.V. Beck, Surface heat flux determination using an integral method, Nuclear Engineering and Design 7 (1968) 170–178.

[17] J.V. Beck, B. Blackwell, C.R.St. Clair, Inverse Heat Conduction: Ill-Posed Problems, Wiley Interscience, New York, 1985.

[18] A.M. Osman, K.J. Dowding, J.V. Beck, Numerical solution of the general two-dimensional inverse heat conduction problem (IHCP), ASME Journal of Heat Transfer 119 (1997) 38–45.

[19] M. Necati Ozisik, H.R.B. Orland, Inverse Heat Transfer, Taylor & Francis, 2000.

[20] F.P. Incropera, D.P. Dewitt, Introduction to Heat Transfer, fourth ed., John Wiley & Sons, 2001.

[21] R. Pasquetti, D. Petit, Inverse heat conduction problems with boundary elements: analysis of a corner effect, Engineering Analysis with Boundary Element 13 (1994) 321–331.